Dipole orientational order at the critical interface

Ashis Mukhopadhyay and Bruce M. Law
Condensed Matter Laboratory, Department of Physics, Kansas State University, Manhattan, Kansas 66506-2601
(Received 12 April 2000; published 20 December 2000)

We present experimental evidence that dipoles exhibit orientational order at the critical interface of mixtures of polar plus nonpolar liquids using the technique of ellipsometry. In this technique the ellipticity $\overline{\rho}$ at the critical interface for all nonpolar or weakly polar fluids or fluid mixtures diverges as $t^{\beta-\nu}$ where $t=(T_c-T)/T_c$ is the reduced temperature relative to the critical temperature T_c and $\beta=0.328, \nu=0.632$ are critical exponents. For polar fluids, however, the dipole-image dipole interaction at the interface can cause long-range orientational order resulting in deviations from this power-law divergence. Theoretical results predict that the surface orientational order parameter $\alpha_2(z)\sim m^{*4}[d^2v(z)/dz^2]$, where m^* is the reduced dipole moment and $v(z)$ is the local composition at position z within the interface. We find quantitative agreement with these predictions for two different critical binary liquid mixtures composed of a highly polar plus nonpolar component.

DOI: 10.1103/PhysRevE.63.011507 PACS number(s): 68.15.+e, 68.35.Rh, 05.70.Jk, 64.60.Fr

I. INTRODUCTION

There are two basic mechanisms which are responsible for long-range orientational order of molecules in the bulk phase of a fluid. In the nematic liquid crystal phase the steric interaction between molecules which possess a highly anisotropic shape, e.g., long rods or flat discs, induces spontaneous orientational order where the long axis of the molecules align approximately parallel to each other. The occurrence of these structures arises primarily from the geometry of the molecules and is a manifestation of the short-ranged repulsive force between the molecules [1]. These molecules are generally large and the dipolar force (discussed below) is relatively weak. Due to the technical importance of these materials, the preferential alignment of such molecules has attracted considerable theoretical and experimental attention [2]. Theoretical calculations indicate that a second type of bulk orientational order can occur in polar fluids due to the presence of the long-range dipolar interaction even in the absence of any anisotropic steric interaction [3]. However, if the polar molecules are small in size and contained in a medium of high static dielectric constant then the dipolar interaction is usually not strong enough, compared with the thermal energy, to lead to any strong mutual ordering of the molecules in the bulk [4]. The molecules are then free to rotate and because the typical rotational time of a molecule is much shorter than the time between two collisions, each molecule experiences a potential due to others which is an average over all orientations. This angle-averaged effective pair-potential $V(r)$ for dipolar molecules is temperature dependent, isotropic, and has the same r^{-6} power dependence as a function of intermolecular distance r as the well-known Lennard-Jones interaction [5]. Thus the bulk behavior of polar fluids usually does not differ much from that of nonpolar fluids.

In this paper we study the orientation of molecules that occurs near an interface. For example, at a lipid-water interface the hydrocarbon chains prefer to align perpendicular to the interfacial plane [6]. The origin of this interaction is the orientation dependent hydrogen bond, commonly known as the hydrophobic interaction. This kind of interaction is short ranged and primarily involves water. In polymer solution, the polymers in the vicinity of an interface exhibit orientational order where molecules are oblate on the polymer-rich side and prolate on the polymer-poor side. This situation becomes much more complex for polymers which posses a distinguishable ''head'' and ''tail,'' for example, polymers with a net dipole moment. In this case both the entropic effect due to the connectivity of the chains and the anisotropic dipole-dipole interaction between two polymers must be considered. This kind of orientational order is coupled to the derivative of the density [7]. The density varies through an interface within a correlation length ξ (of order a molecular size) and the orientation is confined to within a few monolayers of the interface. However, near a continuous phase transition where the width of the (critical) interface ξ diverges, the orientational order can be much more interesting. In this case it is not sufficient to determine the average orientation θ of the molecule with respect to the surface normal (z direction) within the interfacial layer, instead the positional dependence of the orientational order must be taken into account. A simple system in which to study this spatial variation of the orientational order is a critical mixture of a polar and a nonpolar liquid near its phase-separation temperature.

The preferential ordering of the dipoles at the critical interface of a polar and a nonpolar liquid mixture can be qualitatively explained in terms of the interaction between a real dipole and its image dipole. If a real dipole, of dipole moment m and orientation θ with respect to the surface normal, is placed in a medium of static dielectric constant ϵ_{as} at a distance z from the interface then an image dipole, of dipole moment $m(\epsilon_{as}-\epsilon_{bs})/(\epsilon_{as}+\epsilon_{bs})$ and angle $(\pi-\theta)$, appears in the second medium of static dielectric constant ϵ_{bs} at distance $-z$ from the interface [8]. The interaction energy E between the real and image dipole is given by

$$E=-\frac{m^2}{16}\frac{\epsilon_{bs}-\epsilon_{as}}{\epsilon_{as}(\epsilon_{as}+\epsilon_{bs})}\frac{1+\cos^2\theta}{z^3}. \quad (1)$$

This interaction energy is strong near the interface of a polar liquid because all polar solvents possess a high static dielectric constant ($\epsilon_{\text{static}} > 15$) [9]. At a fixed distance z, E is a minimum for $\theta = 0$ or π if $\epsilon_{as} < \epsilon_{bs}$ and for $\theta = \pi/2$ or $3\pi/2$ if $\epsilon_{as} > \epsilon_{bs}$. Therefore the preferred orientation of the dipoles is perpendicular to the interface if the dipole is located in the medium of smaller static dielectric constant or parallel to the interface if the dipole is located in the medium of larger static dielectric constant. Equation (1) illustrates two additional points: (i) the orientational order vanishes as the critical temperature is approached because $\epsilon_{bs} - \epsilon_{as} \sim t^{\beta} \to 0$ as the reduced temperature $t = (T_c - T)/T_c \to 0$ and (ii) there is no orientational order in the bulk ($z \to \pm\infty$) and therefore polar liquids do not exhibit any liquid-crystal-like bulk anisotropy.

An immediate consequence of the presence of surface orientational order is that the anisotropic interface influences both the interfacial tension and the polarization (or ellipticity) of any light reflected from the surface. However, as mentioned above, the modification of the surface properties due to the orientation of dipolar molecules is expected to be important only far from the critical temperature. Numerous experiments have revealed evidence for surface orientational order of dipoles at the liquid-vapor interface far from any critical point [10] generation which determines the average orientation of the molecules within a few monolayers of the interface. Theory indicates, however, that the spatial variation of the orientational order, denoted $\alpha_2(z)$, is important in the vicinity of an interface [11]. There have been few experimental studies which have attempted to quantitatively study these theoretical predictions. We presented evidence for the spatial variation of the ''dipolar'' orientational order at the critical liquid-liquid interface for the ionic mixture triethyl-*n*-hexylammonium triethyl-*n*-hexylboride ($N_{2226}B_{2226}$) in the solvent diphenyl ether (henceforth denoted *NBD*) using the surface sensitive technique of Brewster angle ellipsometry [12]. Our ellipsometric data for this system agreed qualitatively with a model calculation based upon the theoretical results of Frodl and Dietrich [13] who demonstrated that orientational order is present at the critical liquid-vapor interface of dipolar fluids. For the system *NBD* the salt ($N_{2226}B_{2226}$) dissociates in the solvent to form neutral ion pairs with a large dipole moment, therefore, an appropriate analog for an ionic mixture composed of neutral ion pairs is a dipolar fluid. Unfortunately, in this type of system the value of the dipole moment is difficult to determine because the separation distance between the ions is not well known and hence the dipole moment m must be treated as an adjustable parameter. More recently we conducted a more definitive test by investigating the orientational order at the critical interface of a polar plus nonpolar liquid mixture [14], where the polar component possessed a known value for the dipole moment. For these systems a quantitative comparison between theory and experiment is possible with no adjustable parameter. In this publication we shall analyze our ellipsometric data for the critical interface of polar plus nonpolar liquid mixtures to capture the dependence of the orientational order on temperature, dipole strength, and its variation as a function of depth into the interface.

The plan for this paper is as follows. In Sec. II we briefly review the model which describes the spatial variation of the orientational order $\alpha_2(z)$ in the vicinity of the critical interface of a polar plus nonpolar liquid mixture. This function is universal and predicted to vary proportional to the second derivative of the dipolar volume fraction through the interface. Dipoles, in general, possess an anisotropic optical dielectric ellipsoid with principal dielectric constants $(\epsilon_1, \epsilon_2, \epsilon_3)$. If these dipoles are orientationally ordered in the vicinity of an interface then this dielectric ellipsoid for the dipoles gives rise to a local *optical anisotropy* where the dipole dielectric constants parallel $[\epsilon_{\parallel}^{d}(z)]$ and perpendicular $[\epsilon_{\perp}^{d}(z)]$ to the interface are not equal. In Sec. III the factors that contribute to the ellipticity (measured in ellipsometry) for a locally anisotropic interface are described while the experimental results for a number of polar plus nonpolar liquid mixtures are presented and compared with theory in Sec. IV. This paper ends with a discussion (Sec. V) where future experiments which could verify other aspects of the theory are suggested. A number of ancillary results required in the theory or the analysis of the data are derived in the appendixes.

II. INTERFACIAL MODEL

Most microscopic model calculations for fluids are based upon the assumption that the interaction potential between molecules are spherically symmetric and of the Lennard-Jones type [15]. Such a description is only appropriate for isotropic fluids where a scalar order parameter, i.e., the density or the relative density difference is adequate. Molecules typically possess both a shape anisotropy and a permanent dipole moment. Polymers and dipolar molecules in solution are examples of spatially inhomogeneous systems where the local order parameter must take into account the orientation of the molecules. The quantity that describes the spatial variation of orientational order is called the orientational order parameter. It is well known that for inhomogeneity induced orientation, the orientational order parameter is coupled to the derivative of the density [16]. As a consequence near an interface, where there is a variation of density, a nonzero value of the orientational order parameter can be expected. From rather general theoretical considerations if the orientable object can sense the sign of the gradient so that one end of the object prefers to be in contact with a particular phase compared with the other end then the orientational order of the object at the interface will couple to dv/dz, where $v = v(z)$ is the local volume fraction through the interface. An example for this type of surface orientational order is surfactant molecules at a water interface. If, however, the orientable object cannot distinguish z from $-z$, as occurs with polar molecules (because the end group does not prefer a particular phase), then the orientational order of the object couples to $(dv/dz)^2$ and d^2v/dz^2 [16,17].

This coupling between the orientational order and various derivatives of the local volume fraction is evident at polymer interfaces where the orientational order parameter is described by the scalar quantity $S = \langle \cos^2\theta_n - \frac{1}{3} \rangle$ and θ_n is the angle between the z axis and the orientation of the nth monomer. For a polymer-solvent interface a mean-field theory predicts the following z dependence for S [7]:

$$S \sim \left[\frac{d^2 v}{dz^2} - v \frac{dv}{dz} - \frac{2}{3} \left(\frac{dv}{dz} \right)^2 \right], \tag{2}$$

where the proportionality constant is system dependent. The dominant term in Eq. (2) is d^2v/dz^2 (see later), therefore, S is an odd function of z because $v(z)$ is an odd function of z. Equation (2) ultimately implies that bonds are preferentially oriented parallel to the interface in the polymer-rich phase and perpendicular to the interface in the polymer-poor phase [7]. Here the density gradient is the origin of this orientational order, hence, the orientational order will be present even in the absence of any anisotropic interaction amongst the molecules.

A simple model which describes a polar fluid is the Stockmayer model for spherical molecules of hard-sphere diameter σ and dipole moment m. In this model there is both an isotropic Lennard-Jones potential and an anisotropic dipole-dipole interaction between permanent dipoles. Density functional analysis has been used to determine density and orientational order profiles at liquid-vapor, wall-liquid, and wall-vapor interfaces of Stockmayer fluids [18]. Frodl and Dietrich (FD) have developed a density functional theory to investigate the orientational ordering of dipolar molecules near the critical interface of a phase-separated dipolar fluid. Unlike certain earlier theories their approach is reliable even for highly polar fluids. The details of the model and the numerical results are explained in Ref. [13]. In essence, for a laterally isotropic interface the local volume fraction of polar molecules $v(z,\theta)$ is a function of z and angle θ between the z axis and the direction of the dipole moment m of the molecule. $v(z,\theta)$ can be factorized into a total number density $v(z)$ integrated over all orientations and a dimensionless orientational order parameter $\alpha(z,\theta)$ which determines the angular distribution

$$v(z,\theta) = v(z)\alpha(z,\theta)/2\pi, \tag{3}$$

where $\alpha(z,\theta)$ has to satisfy the normalization condition

$$\int_0^\pi \alpha(z,\theta) \sin\theta d\theta = 1. \tag{4}$$

The angular dependence of $\alpha(z,\theta)$ can be expressed in terms of Legendre's polynomials $P_l(\cos\theta)$,

$$\alpha(z,\theta) = \sum_{l=0}^{\infty} \alpha_l(z) P_l(\cos\theta), \tag{5}$$

where $\alpha_0(z) = \frac{1}{2}$ and, in the absence of any external fields, $\alpha_l(z) = 0$ for all odd values of l indicating the absence of any net polarization on either side of the interface. The spatial variation of the orientational order at the interface is therefore described primarily by $\alpha_2(z)$ where α_2 is an odd function of z. It is negative in the dipole-rich phase and positive in the dipole-poor phase corresponding to dipoles which are oriented parallel (perpendicular) to the interface in the dipole-rich (dipole-poor) phase. This description of the dipoles near a critical interface is similar to the description of polymers near an interface which are oblate (parallel to the interface) on the polymer-rich side and prolate (normal to the interface) on the polymer-poor side. α_2 is a measure of the strength of the anisotropic dipolar interaction compared with the isotropic Lennard-Jones interaction. This function possesses two extrema whose amplitude is proportional to m^{*4} where

$$m^* = \frac{m}{\sqrt{\sigma^3 u_0}} \tag{6}$$

is the reduced dipole moment, u_0 is the Lennard-Jones potential well depth, and σ is the average hard-sphere diameter for the dipole. For $m^* > 1$ orientational ordering of dipoles can significantly perturb the interfacial behavior of polar fluids. From their density functional calculation FD obtained the following scaling form for $\alpha_2(z,t)$ [13]:

$$\alpha_2(z,t) \sim t^{\beta+2\nu} Y(z/\xi), \tag{7}$$

where $\xi = \xi_{0-} t^{-\nu}$ is the bulk correlation length in the two-phase region. The numerical technique used by FD could not provide an explicit analytic expression for the function $Y(z/\xi)$. Following a suggestion of Sluckin [19] it seems probable that the function $Y(z/\xi)$ is proportional to the second derivative of the composition profile $v(z)$ through the critical interface, hence, in our calculations we have assumed that

$$\alpha_2(z,t) = \frac{D\xi_{0-}^2 m^{*4}}{\Psi_0} \frac{d^2 v}{dz^2} \sim t^{\beta+2\nu}, \tag{8}$$

where Ψ_0 is the coexistence curve amplitude and D is a dimensionless constant whose value is selected to provide numerical agreement with the amplitude of α_2 deduced from the mean-field density functional calculations of Frodl and Dietrich [13]. In mean-field theory the local order parameter through the critical interface is described by [20]

$$\Psi(z,t) = v(z) - v_c = \Psi_0 t^\beta \tanh(z/2\xi), \tag{9}$$

where v_c is the critical composition of the polar component. We demonstrated earlier [12] that for $m^* = 1.5$ and $t = 0.01$ the value $D = 0.2402$ provided excellent agreement between Eq. (8), with $v(z)$ given by Eq. (9), and the mean-field density functional calculations of Frodl and Dietrich. Equation (8) therefore provides not only the appropriate positional dependence but also the appropriate reduced temperature dependence predicted by Frodl and Dietrich. The shape of $\alpha_2(z)$ as a function of z is shown in Fig. 1 (solid line) where $m^* = 1.5$ and $t = 0.01$. The small magnitude for the orientational order parameter $[\alpha_2(z)|_{\max} \sim 2 \times 10^{-4}]$ compared with the isotropic background represented by $\alpha_0 = \frac{1}{2}$ and the temperature dependence of $\alpha_2(z)$ [Eq. (8)] indicates that orientational ordering effects will only be evident at the critical-liquid–liquid interface at large reduced temperatures provided a highly surface-sensitive experimental technique is used even for molecules possessing a large dipole moment.

An alternative form which could provide a description of the orientational order parameter α_2 might be the function S given in Eq. (2) as suggested by Widom [16]. S and α_2 are compared in Fig. 1 where S (dashed line) has been rescaled to provide the same absolute magnitude at the peak. S and α_2 can barely be distinguished because d^2v/dz^2 is the dominant

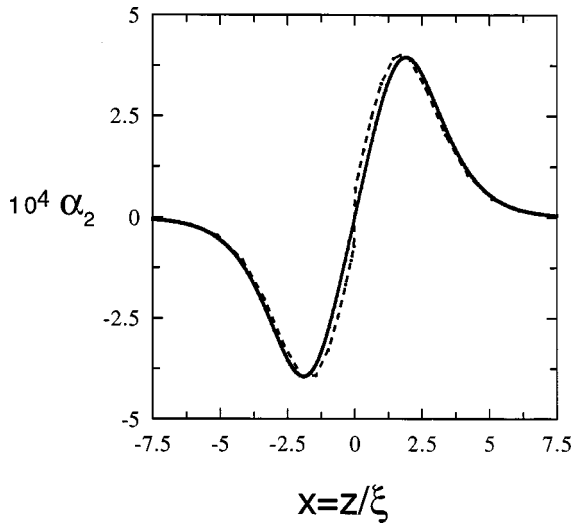

FIG. 1. Comparison of our ansatz for the orientational order parameter α_2, as given by Eq. (8) (solid line), with the scaled Carton and Leibler function [7] [Eq. (2), dotted line] which describes the orientational order for polymers at a polymer-solvent interface.

term in Eq. (2). Therefore, later in this paper, we also consider S as a possible contender for describing the orientational order at an interface.

Dipolar model. Most molecules which possess a permanent dipole moment are nonspherical in shape and have an anisotropic optical polarizability [5] represented by the dipole's optical dielectric ellipsoid $(\epsilon_1,\epsilon_2,\epsilon_3)$ where the ϵ_1 axis is chosen to point along the dipole moment m direction. Near an interface, if the dipole becomes orientationally ordered then the local dielectric constant at depth z will be anisotropic with differing values parallel $[\epsilon_{\|}(z)]$ and perpendicular $[\epsilon_{\perp}(z)]$ to the interface. This local optical dielectric anisotropy influences the ellipticity of light reflected from this interface. We expect $\epsilon_{\|}(z)$ and $\epsilon_{\perp}(z)$ are related to the dielectric ellipsoid $(\epsilon_1,\epsilon_2,\epsilon_3)$, the orientational order parameter $\alpha(z,\theta)$ [Eq. (5)], and the local dipolar volume fraction $v(z)$ through the interface.

Before discussing the dielectric properties within a polar plus nonpolar mixture $[\epsilon_{\|}(z)$ and $\epsilon_{\perp}(z)]$ we first consider the dielectric properties of an oriented dipole where a superscript d will refer to a dipolar property. For a dipole oriented at angle θ to the z axis, the parallel and perpendicular components of the dipole's dielectric constant are given, respectively, by (see Appendix A)

$$\epsilon_{\perp}^{d}(\theta)=\frac{1}{\sqrt{\left(\frac{\cos^2\theta}{\epsilon_1}+\frac{\sin^2\theta}{\epsilon_2}\right)\left(\frac{\cos^2\theta}{\epsilon_1}+\frac{\sin^2\theta}{\epsilon_3}\right)}} \tag{10}$$

and

$$\epsilon_{\|}^{d}(\theta)={}_2F_1\sqrt[4]{\frac{\epsilon_2\epsilon_3}{\left(\frac{\sin^2\theta}{\epsilon_1}+\frac{\cos^2\theta}{\epsilon_2}\right)\left(\frac{\sin^2\theta}{\epsilon_1}+\frac{\cos^2\theta}{\epsilon_3}\right)}}. \tag{11}$$

At a particular depth z the orientational order parameter $\alpha(z,\theta)$ describes the distribution in orientations therefore the angle-averaged dipole dielectric constants parallel $[\epsilon_{\|}^{d}(z)]$ and perpendicular $[\epsilon_{\perp}^{d}(z)]$ to the interface can be calculated from

$$\epsilon_{\|(\perp)}^{d}(z)=\int_0^{\pi}\epsilon_{\|(\perp)}^{d}(\theta)\,\alpha(z,\theta)\sin\theta\,d\theta. \tag{12}$$

For isotropic molecules or randomly oriented dipoles [where $\alpha(z,\theta)=\frac{1}{2}$] Eq. (12) reduces to $\epsilon_{\|}^{d}(z)=\epsilon_{\perp}^{d}(z)=\epsilon^{d}(z)$, as expected. If, however, the dipoles are preferentially oriented at the interface then in general $\epsilon_{\|}^{d}(z)\neq\epsilon_{\perp}^{d}(z)$ and the interface is locally *anisotropic*.

At depth z within the interface the local volume fraction $v(z)$ of dipoles is also a function of position. Hence the parallel $[\epsilon_{\|}(z)]$ and perpendicular $[\epsilon_{\perp}(z)]$ dielectric constants through the interface for a solution can be obtained from the two component Clausius-Mossotti relation [21]

$$F[\epsilon_{\|(\perp)}(z)]=v(z)F[\epsilon_{\|(\perp)}^{d}(z)]+[1-v(z)]F(\epsilon_s), \tag{13}$$

where $F(x)=(x-1)/(x+2)$ and ϵ_s is the optical dielectric constant of the nonpolar component.

In mean-field theory the local volume fraction $v(z)$ through the interface is described by Eq. (9). If fluctuations are important (i.e., for real fluids) then the intrinsic order parameter profile is instead described by

$$\Psi(z)=v(z)-v_c=\Psi_0 t^{\beta} f(z/2\xi), \tag{14}$$

where the well-known Fisk-Widom function [22]

$$f(x)=\frac{\sqrt{2}\tanh(x)}{\sqrt{3-\tanh^2(x)}}. \tag{15}$$

Equations (10)–(15) and (8) provide a description of how the optical dielectric anisotropy is predicted to vary as a function of position through a critical interface. These equations are used in the next section for comparing theory with experiment.

III. EXPERIMENTAL TECHNIQUE

Phase-modulated ellipsometry is a particularly effective and convenient method for probing surface structure. It has been used for many years to probe the interfacial structure in a large variety of systems [23]. In this paper we use this technique to study dipole-induced surface orientational order at the critical interface of mixtures composed of a polar and a nonpolar component. In this technique we measure the ellipticity $\overline{\rho}=\mathrm{Im}(r_p/r_s)_{\theta_B}$, which is the imaginary component of the ratio of the complex reflection amplitudes at the Brewster angle θ_B where $r_p(r_s)$ is the reflection amplitude for $p(s)$ polarization. At the Brewster angle the Fresnel contribution from the bulk media vanishes and $\overline{\rho}$ entails only surface contributions. For a critical interface there are two contributions from the intrinsic order parameter profile [Eqs. (14) and (15)] and from thermally generated capillary waves (which roughen the interface). The intrinsic component of $\overline{\rho}$ for a thin (compared to the wavelength of light λ) and lo-

cally anisotropic interface is described by [24]

$$\bar{\rho}_{\rm int}=\frac{\pi}{\lambda}\frac{\sqrt{\epsilon_a+\epsilon_b}}{\epsilon_a-\epsilon_b}\int \epsilon_{\parallel}(z)+\frac{\epsilon_a\epsilon_b}{\epsilon_{\perp}(z)}-(\epsilon_a+\epsilon_b)dz, \quad (16)$$

where $\epsilon_a=n_a^2(\epsilon_b)$ is the optical dielectric constant in the incident (reflected) medium while $\epsilon_{\parallel}(z)$ and $\epsilon_{\perp}(z)$ are the dielectric profiles through the interface [Eq. (12)]. To first order in $\Delta\epsilon=\epsilon_a-\epsilon_b$ the capillary wave contribution to $\bar{\rho}$ for an isotropic interface is given by [12]

$$\bar{\rho}_{\rm cap}=\sqrt{2}\,\frac{\pi}{\lambda}\xi(n_a-n_b)\frac{1}{32\pi R}\int_{-\infty}^{\infty}\frac{dK}{2\pi}[|\phi_{\parallel}(K)|^2 + 2|\phi_{\perp}(K)|^2]\ln[1+(2a_0/K)^2], \quad (17)$$

where $R=0.128$, $a_0=0.748$, and $\phi_{\parallel}(K)[\phi_{\perp}(K)]$ is proportional to the inverse Fourier transform of the derivative of $\epsilon_{\parallel}(z)[\epsilon_{\perp}(z)]$. Marvin and Toigo have shown that if both the interfacial thickness and the mean capillary wave amplitude are much smaller than the wavelength of light then these two contributions are additive, $\bar{\rho}=\bar{\rho}_{\rm int}+\bar{\rho}_{\rm cap}$ [25].

If the interface is locally isotropic, so that $\epsilon_{\parallel}(z)=\epsilon_{\perp}(z)$, then Eqs. (16) and (17) reduce to [26]

$$\bar{\rho}=\frac{\sqrt{2}\pi}{\lambda}\xi\Delta n|\eta_D+\eta_R|, \quad (18)$$

where $\Delta n=|n_b-n_a|$ is the refractive index difference between the two bulk phases

$$\eta_D=\int_{-\infty}^{\infty}[1-f^2(x)]dx, \quad (19)$$

where $f(x)$ is given by Eq. (15) and

$$\eta_R=\frac{3}{32\pi R}\int_{-\infty}^{\infty}\frac{dK}{2\pi}|\phi(K)|^2\ln[1+(2a_0/K)^2], \quad (20)$$

where $\phi(k)$ is the inverse Fourier transform of the derivative of $f(x)$. Both η_D and η_R are universal numbers because these quantities involve integrations over the universal order-parameter profile $f(x)$ at the interface. For the Fisk-Widom profile [Eq. (15)] they take the values $\eta_D=2.28$ and $\eta_R=0.77$. Therefore for a locally isotropic interface, according to Eq. (18), the ellipticity $\bar{\rho}\sim t^{\beta-\nu}$ diverges on approaching the critical temperature because $(n_b-n_a)\sim t^{\beta}$ and $\xi\sim t^{-\nu}$ where the critical exponents $\beta=0.328$ and $\nu=0.632$ for Ising mixtures [27]. It is important to note that the reduced temperature dependence $\bar{\rho}\sim t^{\beta-\nu}$ is independent of the specific form assumed for the universal interfacial profile $f(x)$ because $f(x)$ only influences the values of the universal numbers η_D and η_R. Schmidt and co-workers have made the most detailed experimental study of (isotropic) critical interfaces and found excellent agreement with the predicted $\bar{\rho}\sim t^{\beta-\nu}$ divergence for binary liquid mixtures [28], polymer solutions [29], and pure fluids [30]. Their experimental results are in quantitative agreement with the theoretical result given in Eq. (18) with no adjustable parameters [26]. At the time it was not realized that the effects of surface anisotropy might be evident at very large reduced temperatures t (~ 0.1) for polar systems and polymer solutions; the systems were primarily studied at small reduced temperatures ($t \lesssim 0.05$) where orientational ordering effects at the critical interface are not expected to be very large.

IV. EXPERIMENTAL RESULTS

What are the optimal characteristics for systems which are expected to exhibit dipole-induced surface orientational order at the critical interface of a binary liquid mixture? According to Eq. (8), where $\alpha_2\sim m^{*4}$, and the definition of the reduced dipole moment m^* [Eq. (6)] the dipole should possess a large dipole moment m and a small hard-sphere diameter σ while at the same time having a large molecular optical dielectric anisotropy so that any dipole orientational order strongly influences the ellipticity of the light reflected from the critical interface. All of these molecular characteristics for the dipole should be known so that there are no adjustable parameters. Another important characteristic for the polar component is that it should not self-associate in the bulk; self-association such as occurs in many hydrogen bonding liquids such as water will produce clusters of molecules with ill-defined effective dipole moments and effect dielectric anisotropies. The Kirkwood correlation factor g_K, which reflects the degree of correlation between the orientations of neighboring molecules, should be approximately 1.0 [31]. It is preferrable if the second component of the liquid mixture is nonpolar and optically isotropic so that this component possesses no tendency to either orient at the interface or orient in the vicinity of the dipolar component. The orientational order parameter $\alpha_2\sim t^{\beta+2\nu}$ [Eq. (8)], hence, the orientational order is only expected to be prevalent at large reduced temperatures t. Therefore the polar plus nonpolar critical mixture should also possess a readily accessible critical temperature and large two-phase region so that phenomena at large $t(\sim 0.1)$ can be studied.

In this paper we study the following nonpolar plus polar critical mixtures which largely conform with the above requirements: two nonpolar plus highly polar mixtures, carbon disulphide + acetonitrile (CA) and cyclohexane + 2-nitroanisole (CN), and one nonpolar plus weakly polar mixture, carbon disulphide + methanol (CM). The molecular properties for the polar component are listed in Table I while relevant characteristics of the critical liquid mixture are listed in Table II. The determination of some of these parameters are discussed later in this section and in the appendixes to this paper. Acetonitrile will not be strongly structured in the bulk as it possesses a Kirkwood correlation factor of $g_K=1.09$ [31], however, by comparison methanol is expected to form chains in solution ($g_K=3.25$ [31]) but its small reduced dipole moment ($m^*\sim 1$) will not lead to significant orientational order in the vicinity of the interface.

All chemicals used in the preparation of these mixtures were purchased from Aldrich Chemical company and possessed a purity of better than 99%. The carbon disulphide, although it had a reported purity of 99.9+%, appeared yellow. It was therefore doubly distilled before use. The critical liquid mixtures were contained in a well-annealed 20 c.c. cylindrical pyrex sample cell of length 8 cm where the cell was filled sufficiently so that the critical-liquid–liquid inter-

TABLE I. Dipolar parameters.

	2-nitroanisole	acetonitrile	methanol
$\sigma(nm)$	0.65	0.45–0.50	0.38–0.46
$u_0\times10^{21}(J)$	2.68-2.83	3.33-3.71	3.94–4.44
$m(D)$	4.51	3.52	1.61
$m^*(\text{est})=m/\sqrt{\sigma^3 u_0}$	1.59-1.64	1.65-2.00	0.75-1.08
$m^*(\text{expt})$	1.81	2.23	
Principal dielectric constants[a]			
ε_1	3.17	2.45	1.99
ε_2	2.64	1.55	1.73
ε_3	1.73	1.55	1.57

[a]Calculation of the principal dielectric constants for 2-nitroanisole is described in Appendix A. For acetonitrile ϵ_1 is choosen in the direction of the dipole moment and the same procedure was followed as described in Appendix A. For methanol the values are taken from Ref. [50].

face appeared approximately in the middle of the sample cell. A small gas bubble was retained in the cell to prevent breakage at high temperatures. Prior to filling the cell, the interior was etched clean for 60 sec using the following glass etching solution: 5% HF, 35% HNO_3, and 60% H_2O by volume. It was then rinsed well in distilled deionized water and dried at a high temperature. The cylindrical axis of the sample cell was oriented horizontally and concentrically inside a two-shell cylindrical thermostat where the incident and reflected laser beams from the ellipsometer are normal to windows on the thermostat and to the sample cell Pyrex surface. The thermostat consisted of an inner resistively heated aluminum shell and an outer water and antifreeze cooled brass shell where the heater wires and cooling tubes were carefully designed to minimize the presence of any thermal gradients along the length of the oven. At very low temperatures, below the dew point, the thermostat was enclosed inside an additional dry atmosphere bag which contained curved glass windows through which the laser beam could propagate. The thermostat has a temperature stability of ~1 mK over 4 h. Precision thermistors monitored the temperature at both ends of the sample cell; gradients along the cell were maintained at less than 1 mK/cm. The critical temperature for each mixture was determined within the thermostat by observing the spinoidal ring as the sample was slowly cooled into the two phase region. This technique usually determined T_c to within a few mK [32].

The phase-modulated ellipsometer used in all of the measurements is similar in design to that used by Beaglehole

TABLE II. Critical liquid mixture properties.

	v_c^a	T_c(K)	Ψ_0	ξ_{0-}(nm)
CN	0.336	345.05	0.85	0.125
CA	0.396	323.54	0.73	0.1
CM	0.33	309.50	0.59	0.177

[a]Volume fraction of the polar component: 2-nitroanisole for CN, acetonitrile for CA, and methanol for CM.

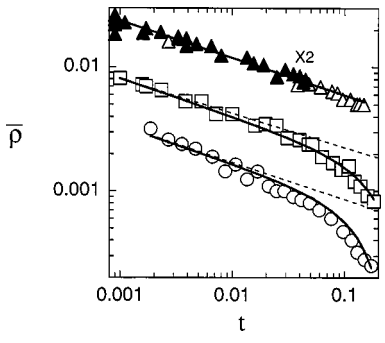

FIG. 2. Log-Log plot of ellipticity $\overline{\rho}$ versus reduced temperature t for carbon disulphide + methanol (CM, triangles), carbon disulphide + acetonitrile (CA, squares), and cyclohexane + 2-nitroanisole (CN, circles). The solid (open) triangles for CM are from Ref. [28] (our measurements). The error bar for each data point is $\pm5\times10^{-5}$. The solid lines for CA and CN data are from theory, as described in the text, using the parameters given in Tables I and II. The dashed lines represent the ellipticity in the absence of surface orientation order ($\alpha_2=0$).

[24] where an essential feature which guarantees the stability of the measurements is the use of an ultrastable birefringence modulator [33]. Our measurement procedure consisted of setting the temperature, waiting for thermal and diffusive equilibrium, and then taking 20($\overline{\rho}$,t) measurements over the period of an hour. Each datum point is then represented by the average $\overline{\rho}$ and t value of these twenty measurements. Initially we monitored $\overline{\rho}$ continuously for 24 h to check the wait time necessary before taking measurements. The typical wait time for diffusive equlibrium was 6 h beyond the establishment of thermal equlibrium, at least, far from T_c. Near T_c this wait time was increased to as much as 12 h to account for the ''critical slowing down'' of the sample. The standard deviation for a single $\overline{\rho}$ datum point is of order 2×10^{-5}. Several runs were taken on all samples where the temperature was always decreased so that gravity assisted the phase separation process. Different runs showed a typical reproducibility of $\pm5\times10^{-5}$ in $\overline{\rho}$.

As discussed in Sec. I polar molecules in a medium of high static dielectric constant can rotate freely and thus experience an angle-averaged potential due to other molecules which varies as $V(r)\sim-(1/r)^6$. It has been well established theoretically that if $V(r)\sim-(1/r)^p$ then the critical exponents exhibit Ising values for $p>4.97$ and mean-field values for $p<4.5$ [34]. Both the Lennard-Jones interaction and the rotationally averaged dipole-dipole interaction have $p=6$ and the bulk critical behavior of polar plus nonpolar mixtures is expected to be Ising-like. If the interface is locally isotropic we expect that $\overline{\rho}\sim t^{\beta-\nu}$, where $\beta-\nu=-0.304$ as discussed in Sec. III. In Fig. 2 we show the $\overline{\rho}$ data as a function of the reduced temperature t for the three critical liquid mixtures. The dashed lines represent the results in the absence of any surface anisotropy ($\alpha_2=0$) where $\overline{\rho}=\overline{\rho}_{\text{int}}+\overline{\rho}_{\text{cap}}$ diverges proportional to $t^{\beta-\nu}$. All three critical liquid mixtures follow this temperature dependence at sufficiently small t where the surface orientational order is expected to vanish, however, at

large reduced temperatures ($t \gtrsim 0.1$) the two very polar liquid mixtures, CA (squares) and CN (circles), deviate significantly from this isotropic behavior thus indicating the presence of a surface optical anisotropy. However, the weakly polar liquid mixture, CM (triangles), deviates very little from the isotropic behavior ($\bar{\rho} \sim t^{\beta-\nu}$) even out to a reduced temperature of $t \sim 0.1$. Calculations for this liquid mixture, using the information for the weakly polar molecule methanol provided in Table I, indicate that $\bar{\rho}$ deviates from $t^{\beta-\nu}$ behavior by less than 0.6% at $t=0.1$. Such a small deviation is below the accuracy of the $\bar{\rho}$ measurements in Fig. 2.

In order to quantitatively explain the deviations of the mixtures CN and CA from isotropic behavior at large reduced temperatures ($t \sim 0.1$) various dipole parameters and mixture parameters (which are listed in Tables I and II) must be accurately measured or estimated from other data. We briefly address these issues before continuing our discussion of dipole-induced surface orientational order at the critical interface.

The mixture parameters Ψ_0 and ξ_{0-} are required in the analysis below. The coexistence curve amplitude Ψ_0, for the mixtures CN and CA, was determined by fitting the phase separation temperatures for eight samples of varying volume fraction between 0.1 and 0.9 for each mixture to the coexistence curve $\Psi = |v - v_c| = \Psi_0 t^{\beta}$. Corrections to simple scaling [35] were ignored. The (one-phase) correlation length amplitude ξ_0 is frequently determined from turbidity measurements near the critical temperature. This amplitude, determined from the turbidity, can be rather sensitive to the accuracy of the data, background terms, and small shifts in the assumed critical temperature (see, for example, Table III in Ref. [36]). We therefore prefer an alternative method for finding ξ_0. At small small $t (t < 0.01)$ the ellipticity varies as $\bar{\rho} \sim t^{\beta-\nu}$, hence, Eq. (18) can be used to determine ξ_{0-} once Ψ_0 has been measured. The refractive index coexistence curve Δn, used in Eq. (18), is related to the volume fraction coexistence curve represented by Ψ by the corresponding two component Clausius-Mossotti relation [Eq. (13) with $z \rightarrow \pm\infty$].

The dipole parameters ($\epsilon_1, \epsilon_2, \epsilon_3$), σ, u_0, and m are also required in the analysis below. The principal values of the dielectric constants for the dipole ($\epsilon_1, \epsilon_2, \epsilon_3$) were obtained by calculating the optical polarizabilities of the polar molecule by either adding its bond polarizabilities or, in some cases, by adding its group polarizabilities and then using the Lorenz-Lorentz relation to obtain the optical dielectric constants [37]. An example of this calculation is provided in Appendix A for the molecule 2-nitroanisole. There are many uncertainties in calculating the hard sphere diameter σ, interaction well depth u_0, and dipole moment m within a particular solvent. The methods and uncertainties for calculating these parameters are discussed in Appendix C for the specific example of 2-nitroanisole. The range in values for the dipole parameters given in Table I reflects the uncertainty in these calculations.

We are now in a position to compare the ellipsometric $\bar{\rho}$ data for CN and CA (circles and squares, respectively, in Fig. 2) with the theory for dipole-induced surface orientational order. The solid lines in Fig. 2 were calculated from Eqs. (16) and (17) where $\epsilon_{\parallel}(z)$ and $\epsilon_{\perp}(z)$ were determined from Eqs. (10)–(15) with the orientational order parameter α_2 given by Eq. (8). The only adjustable parameter used in this calculation was the reduced dipole moment $m^*(\text{expt})$. The good agreement between theory and experiment displayed in Fig. 2 was obtained with $m^*(\text{expt}) = 1.81$ and 2.23 for, respectively, the liquid mixtures CN and CA. These values are $\sim 15\%$ higher than the range of values displayed in Table I [$m^*(\text{est})$] estimated using the methods discussed in Appendix C. This can be considered as good agreement between theory and experiment. One should not expect exact agreement because the theory assumes that real dipoles can be approximated by spherical point dipoles possessing a hard sphere diameter of σ and dipole moment m. Real dipoles are usually ellipsoidal in shape where the dipole charge is distributed in space and the repulsive interaction is not normally that of a hard sphere [31].

The orientational order parameter S [Eq. (2)] which possesses a qualitatively similar shape to α_2 (Fig. 1) might also be expected to provide a reasonable description of the experimental ellipsometric $\bar{\rho}$ data. If Eq. (2) is suitably scaled to exhibit the same peak value as in Fig. 1 and used to describe the orientational order parameter α_2, rather than the ansatz given in Eq. (8), then a similar agreement can be obtained between theory and experiment for the mixture CA but with $m^*(\text{expt}) = 2.32$. This value is slightly larger than the corresponding value produced using the ansatz in Eq. (8) [for which $m^*(\text{expt}) = 2.23$]. Perhaps Eq. (8) provides a better model for the orientational order parameter α_2 than Eq. (2), however, this result should be treated with caution considering the approximations used in modeling the dipole and the uncertainties in m^* as discussed in Appendix C.

Finally we note that deviations from $\bar{\rho} \sim t^{\beta-\nu}$ behavior occur only at large reduced temperatures ($t \gtrsim 0.1$) where Ising critical exponents may no longer be strictly applicable. In this regime, if the power law forms $\Psi = \Psi_0 t^{\beta}$ and $\xi = \xi_{0-} t^{-\nu}$ are used, β and ν usually show effective values which are between mean-field and Ising critical exponents. A crossover to mean-field behavior would lead to $\beta = \nu = 0.5$ so that $\bar{\rho} \sim t^{\beta-\nu}$ would level off at large t. Such a leveling off is not apparent for the mixture CM at large t (Fig. 2, triangles); hence a transition to mean field behavior does not appear to be important. (Recall that for the mixture CM surface orientational order effects are expected to be small.)

V. DISCUSSION

In this paper ellipsometry was used to study dipole-induced orientational order at the critical interface of three different nonpolar plus polar binary liquid mixtures. For the weakly polar mixture, cyclohexane + methanol (CM), where the reduced dipole moment $m^* \sim 1.0$ no orientational ordering effects were observed in the ellipticity $\bar{\rho}$ in agreement with theoretical expectations. In this case, and for completely nonpolar mixtures, the critical interface is locally isotropic, namely, $\epsilon_{\parallel}(z) = \epsilon_{\perp}(z)$ where $\epsilon_{\parallel}(z)[\epsilon_{\perp}(z)]$ is the optical dielectric constant parallel (perpendicular) to the interface at

depth z within the interface. The ellipticity under these circumstances exhibits a power law divergence $\bar{\rho} \sim t^{\beta-\nu}$. For two highly polar liquid mixtures, carbon disulphide + acetonitrile (CA) and cyclohexane + 2-nitroanisole (CN) with reduced dipole moments of, respectively, $m^* \sim 1.8$ and ~ 2.2 for the polar component, significant deviations from the power law divergence $\bar{\rho} \sim t^{\beta-\nu}$ were observed at large reduced temperatures $t \gtrsim 0.1$. This deviation indicates the presence of a local surface anisotropy where $\epsilon_{\parallel}(z) \neq \epsilon_{\perp}(z)$ within a correlation length ξ of the interface. The experimental results for these two mixtures are in reasonable quantitative agreement with the theoretical prediction that the local surface orientational order parameter $\alpha_2(z) \sim m^{*4}[d^2 v(z)/dz^2]$ [Eq. (8)] where $v(z)$ is the local dipolar volume fraction through the interface. Other theories suggest that terms such as $[dv(z)/dz]^2$ may occasionally be important, however, the term $d^2 v(z)/dz^2$ always seems to be the dominant contribution to $\alpha_2(z)$.

There may be other methods to test this elegant coupling between the local volume fraction order parameter $v(z)$ and the local orientational order parameter $\alpha_2(z)$. Orientational order at surfaces is now routinely measured using nonlinear optical techniques, such as second harmonic generation. This technique has been used for organic-liquid–liquid interface using infrared light far from the absorption bands of the bulk liquids [38]. Alternatively one can use x-ray reflectometry which also can potentially determine the surface orientational order at liquid-liquid interfaces [39].

Under special circumstances it could be possible to probe the coupling between $\alpha_2(z)$ and $v(z)$ using appropriate molecular tricks. For example, the 2-nitroanisole used in this paper is the first member of a family of nitroanisoles (2-, 3-, and 4-nitroanisole). The dipole moment systematically changes within this family while at the same time the dielectric anisotropy and the hard-sphere diameter remain essentially unchanged; this family would be an ideal probe of Eq. (8). Unfortunately the chemistry of 4-nitroanisole plus cyclohexane is sufficiently different (from 2-nitroanisole plus cyclohexane) that this mixture freezes before one can get to sufficiently large reduced temperatures where orientational ordering effects are important. However, an analogous idea may be possible with other families of molecules.

Equations (8), (16), and (17) actually predict a far wider range in behavior for the ellipticity $\bar{\rho}$ than displayed in Fig. 2. The various types of behavior that can occur under differing conditions are schematically depicted in Fig. 3. A qualitative understanding of the significance of the various curves in Fig. 3 can be obtained by concentrating on the intrinsic contribution [Eq. (16)] which, as mentioned in a previous publication [12], makes the dominant contribution to the ellipticity. For a locally isotropic interface $[\epsilon_{\parallel}(z) = \epsilon_{\perp}(z) = \epsilon(z)]$ Eq. (16) reduces to the Drude equation [40]

$$\bar{\rho}_{\rm int} = \frac{\pi}{\lambda} \frac{\sqrt{\epsilon_a + \epsilon_b}}{\epsilon_a - \epsilon_b} \int \frac{[\epsilon(z) - \epsilon_a][\epsilon(z) - \epsilon_b]}{\epsilon(z)} dz \qquad (21)$$

$$\sim t^{\beta-\nu}, \qquad (22)$$

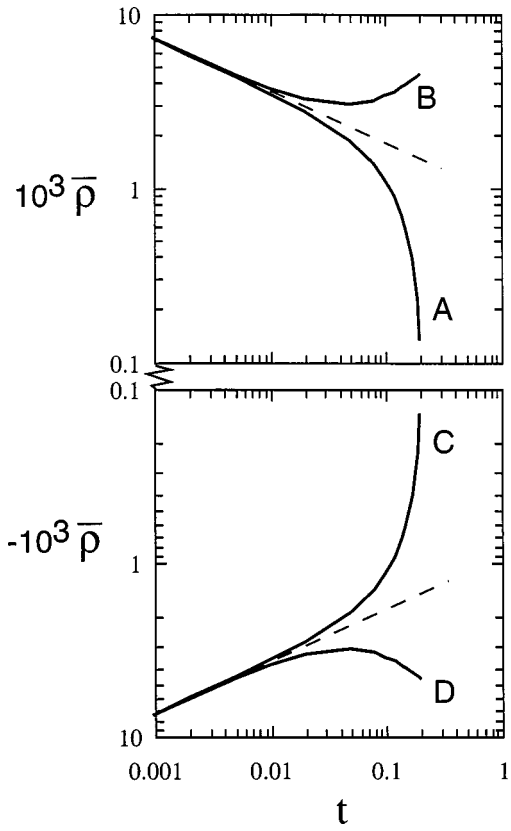

FIG. 3. Schematic diagram of the behavior of the ellipticity $\bar{\rho}$ versus reduced temperature t as a function of various system and dipole parameters. For medium optical dielectric constants $\epsilon_a < \epsilon_b$ then $\bar{\rho}$ is positive (curves A and B) while for the converse case $\bar{\rho}$ is negative (curves C and D) where $\epsilon_a(\epsilon_b)$ is for the incident (reflected) medium. If the dipole possesses a prolate optical dielectric ellipsoid $(\epsilon_1 > \epsilon_2, \epsilon_3)$ the ellipticity is monotonic (curves A and C) while for an oblate optical dielectric ellipsoid $(\epsilon_1 < \epsilon_2, \epsilon_3)$ the ellipticity exhibits an extremum as a function of t (curves B and D).

where the second line above is a reminder that a locally isotropic critical interface (i.e., all critical interfaces sufficiently close to T_c) exhibit this type of power law divergence. In the power law region, if $\epsilon_a < \epsilon_b$, then according to Eq. (21), $\bar{\rho}$ is positive because $\epsilon_a < \epsilon(z) < \epsilon_b$ for all z and the integrand in Eq. (21) is negative. The condition $\epsilon_a < \epsilon_b$ is valid for curves A and B in Fig. 3. If, however, $\epsilon_a > \epsilon_b$ then $\bar{\rho}$ will be negative in the power law region (curves C and D in Fig. 3). The behavior of $\bar{\rho}$ in the locally anisotropic regime, where Eq. (16) must be used, is determined by the shape of the dielectric ellipsoid. For a prolate dielectric ellipsoid where $\epsilon_1 > \epsilon_2, \epsilon_3$ (i.e., the polarizability is greatest along the dipole axis compared with perpendicular to the dipole axis) the ellipticity is monotonic (curves A and C in Fig. 3) while for the converse case of an oblate dielectric ellipsoid $(\epsilon_1 < \epsilon_2, \epsilon_3)$ the ellipticity exhibits an extremum as a function of t (curves B and D in Fig. 3). For most molecules the polarizability along the dipole axis will be larger than the polarizability perpendicular to this axis $(\epsilon_1 > \epsilon_2, \epsilon_3)$ and the ellipticity will be monotonic as a function of t. This is the case for the dipoles considered in this pub-

lication which corresponded to curve A in Fig. 3. There may, however, be other types of unusual dipoles where $\epsilon_1 < \epsilon_2, \epsilon_3$ for which the ellipticity is predicted to exhibit an extremum.

For critical binary liquid mixtures where both components are polar the surface orientational ordering effects could become very complicated and the experimental signal may be difficult to interpret. For example, in Ref. [12] it is believed that the polar solvent diphenyl ether became orientationally order around the pseudodipoles formed from the salt $N_{2226}B_{2226}$ in solution. This ''superdipole'' structure, consisting of a dipole and oriented diphenyl ether solvation shell, was thought to orient in the vicinity of the interface where for agreement between theory and experiment $\epsilon_1 < \epsilon_2, \epsilon_3$ so that an extremum is observed in the ellipticity.

Dipole-induced surface orientational order is also expected to be important at noncritical interfaces, such as the interface between a solid or a vapor and the critical binary liquid mixture. At these noncritical interfaces the liquid component possessing the lowest surface energy preferentially adsorbs. This preferential adsorption is called critical adsorption where the concentration profile $v(z)$ in the vicinity of the interface is described by a universal surface scaling function [41–43]. If one of the components is polar then the dipole–image-dipole interaction can cause this component to become orientationally ordered in the vicinity of the interface. In preliminary work at the noncritical liquid-vapor interface we have found that dipoles which are desorbed from this surface (because they possess the higher surface tension) become orientationally ordered parallel to the interface.

There are many other associated problems where one can use a similar formalism, for example, problems involving inhomogeneous liquid crystals interfaces especially the isotropic-vapor or isotropic-wall interface where one frequently finds prenematic [44] or presmectic behavior [45] at this interface. Liquid crystals generally possess both a shape anisotropy and a permanent dipole moment and therefore it would be interesting to study the relative importance of these two properties in determining the surface orientational order by, for example, selecting a molecule of fixed dipole moment and progressively changing the shape anisotropy by adding successive nonpolar subgroups (eg., $-CH_2-$) in a linear chain. Recently the influence of the nonspherical shape of dipolar molecules on the bulk phase diagram has been studied using density functional theory [3], however, these methods have not yet been extended to the interfacial properties of such systems.

ACKNOWLEDGMENTS

This research work was supported by the National Science Foundation through Grant No. DMR-9631133. We would like to thank Professor B. Widom for useful correspondence.

APPENDIX A: CALCULATION OF THE PRINCIPAL DIPOLE DIELECTRIC CONSTANTS

The polarizability of a molecule can be calculated using two principles. (i) On the assumption that the covalent bonds that make up a molecule are independent of each other then the polarizability of that molecule can be obtained by adding the polarizabilities of its constituent bonds. (ii) The polarizability at an angle θ from a chemical bond is given by

$$\alpha_\theta = \alpha_\parallel \cos^2\theta + \alpha_\perp \sin^2\theta, \tag{A1}$$

where $\alpha_\parallel(\alpha_\perp)$ is the polarizability in a direction parallel (perpendicular) to the bond.

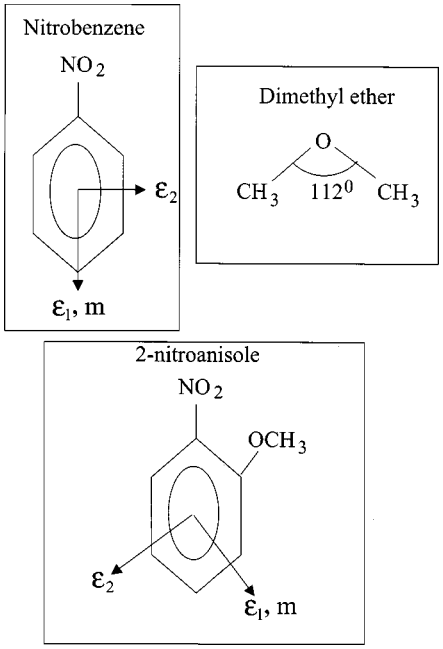

FIG. 4. Schematic structure of the molecules nitrobenzene, dimethyl ether, and 2-nitroanisole which is useful in understanding the calculation of the principal dipole dielectric constants (Appendix A).

As an example of these principles we show how to determine the dipole dielectric ellipsoid for the molecule 2-nitroanisole using the polarizability information available for the molecules nitrobenzene and dimethyl ether. The chemical structure of these molecules is schematically depicted in Fig. 4.

From Ref. [37] the polarizability of nitrobenzene is given by $\alpha_1 = 17.76 \times 10^{-24}$ cm^3 (along the symmetry axis, through the NO_2 group), $\alpha_2 = 13.25 \times 10^{-24}$ cm^3 ($\perp$ to the symmetry axis, in the plane of the benzene ring), and $\alpha_3 = 7.75 \times 10^{-24}$ cm^3 ($\perp$ to the plane of the benzene ring). 2-nitroanisole possesses a methoxy group (-O-CH_3) in its orthoposition. The polarizability of the methoxy group can be obtained by subtracting the contribution of one -CH_3 group from the molecule dimethyl ether (CH_3-O-CH_3) where the polarizability of this molecule has been reported in Ref. [37]. For the methoxy group we find that $\alpha_1 = 3.97 \times 10^{-24}$ cm^3 (through the C-O bond), $\alpha_2 = 2.33 \times 10^{-24}$ cm^3 ($\perp$ to the plane of the methoxy group), and $\alpha_3 = 3.4 \times 10^{-24}$ cm^3 ($\perp$ to the C-O bond, in the plane of the methoxy group).

The polarizability for 2-nitroanisole can therefore be obtained from the polarizability of nitrobenzene by subtracting

the contribution of a C-H group in the orthoposition and adding the polarizability of the methoxy group in this position, hence, $\alpha_1 = 20.57 \times 10^{-24}$ cm^3 (through the NO_2 group), $\alpha_2 = 16.45 \times 10^{-24}$ cm^3 ($\perp$ to the NO_2 group, in the plane of the benzene ring), and $\alpha_3 = 9.5 \times 10^{-24}$ cm^3 ($\perp$ to the plane of the benzene ring).

However, this polarizability for 2-nitroanisole must be recalculated so that α_1 points along the direction of the dipole moment m so that the definition for the optical dielectric constant ϵ_1 agrees with the definition used in this paper. The direction of the dipole moment for 2-nitroanisole can be determined as follows. For isolated molecules, the dipole moment arises from the asymmetric displacement of electrons along the covalent bond, so a characteristic dipole moment can be assigned to each type of covalent bond. The large dipole moment of 2-nitroanisole originates from its two group moments $C^+ - NO_2$ and $C - {}^+OCH_3$ which contribute, respectively, $\approx 3.5D$ and $\approx 1.3D$ [5]. The angle between these two groups is $2\pi/3$. By vectorial summation of these two group moments we obtain the direction of the dipole moment; specifically it makes an angle of approximately 160° to the nitro group. Therefore from Eq. (A1) we obtain $\alpha_1 = 20.86 \times 10^{-24}$ cm^3 (in the direction of the dipole moment), $\alpha_2 = 16.9 \times 10^{-24}$ cm^3 ($\perp$ to the dipole moment, in the plane of the benzene ring), and $\alpha_3 = 9.5 \times 10^{-24}$ cm^3 ($\perp$ to the plane of the benzene ring).

Finally the optical dielectric constant $\epsilon_i (i = 1,2,3)$ can now be obtained from the polarizability α_i using the Lorenz-Lorentz relation

$$\frac{\alpha_i}{4\pi\epsilon_0} = \frac{\epsilon_i - 1}{\epsilon_i + 2} \frac{3v}{4\pi}, \tag{A2}$$

where $v = M/\rho N_0, M$ is the molecular weight, ρ is the mass density, and N_0 is Avogadro's number. Hence we obtain $\epsilon_1 = 3.17, \epsilon_2 = 2.64$, and $\epsilon_3 = 1.73$ which are the values listed in Table I.

APPENDIX B: PARALLEL AND PERPENDICULAR COMPONENTS OF THE DIPOLE DIELECTRIC CONSTANT

For a dipole, whose dipole moment m is oriented at an angle θ relative to the z axis (which also represents the normal to the critical interface), an important relationship exists between the dipole's dielectric constant parallel $[\epsilon_\parallel^d(\theta)]$ or perpendicular $[\epsilon_\perp^d(\theta)]$ to the interface and the dipole's dielectric ellipsoid $(\epsilon_1, \epsilon_2, \epsilon_3)$ where ϵ_1 has been chosen to point along the direction of m. We discuss this relationship in this appendix. It played an important role in our modeling of a locally anisotropic interface in Sec. II.

To find $\epsilon_\parallel^d(\theta)$ and $\epsilon_\perp^d(\theta)$ we use a geometric construction which is commonly used in understanding wave propagation in anisotropic media. Each dipole in solution has a refractive index tensor that can be represented by an ellipsoid with semimajor axes $\sqrt{\epsilon_1}, \sqrt{\epsilon_2}$, and $\sqrt{\epsilon_3}$. The equation which describes this ellipsoid is given by

$$\frac{(x')^2}{\epsilon_3} + \frac{(y')^2}{\epsilon_2} + \frac{(z')^2}{\epsilon_1} = 1, \tag{B1}$$

where $x' = \sqrt{\epsilon}\sin\theta\cos\phi, y' = \sqrt{\epsilon}\sin\theta\sin\phi$, and $z' = \sqrt{\epsilon}\cos\theta$. The z' axis, in the dipole's fixed reference frame, makes an angle (θ, ϕ) to the z axis (which is in the laboratory's fixed reference frame). The perpendicular component of the dipole's dielectric constant is given by the solution of the above equation for ϵ, namely,

$$\epsilon_\perp^d(\theta,\phi) = \frac{1}{\dfrac{\sin^2\theta\cos^2\phi}{\epsilon_3} + \dfrac{\sin^2\theta\sin^2\phi}{\epsilon_2} + \dfrac{\cos^2\theta}{\epsilon_1}}. \tag{B2}$$

A dipole can take any orientation ϕ, hence, averaging over ϕ we obtain

$$\epsilon_\perp^d(\theta) \equiv \langle \epsilon_\perp^d(\theta) \rangle_\phi = \frac{1}{\sqrt{\left(\dfrac{\cos^2\theta}{\epsilon_1} + \dfrac{\sin^2\theta}{\epsilon_2}\right)\left(\dfrac{\cos^2\theta}{\epsilon_1} + \dfrac{\sin^2\theta}{\epsilon_3}\right)}}. \tag{B3}$$

For the special case of a prolate spheroid where $\epsilon_2 = \epsilon_3 \neq \epsilon_1$ we obtain

$$\langle \epsilon_\perp^d(\theta) \rangle_\phi = \frac{\epsilon_1\epsilon_2}{\epsilon_2\cos^2\theta + \epsilon_1\sin^2\theta} \tag{B4}$$

in accord with the result in Ref. [12].

In a similar fashion by taking the projection of the ellipsoid on the XY plane and averaging over ϕ the parallel component of the dielectric constant is

$$\epsilon_\parallel^d(\theta) = \frac{2}{\pi}\epsilon(\theta)\epsilon_2\epsilon_3 \int_0^{\pi/2} \frac{d\phi}{\sqrt{[\epsilon_2\epsilon_3\cos^2\phi + \epsilon(\theta)\epsilon_3\sin^2\phi][\epsilon_2\epsilon_3\cos^2\phi + \epsilon(\theta)\epsilon_2\sin^2\phi]}}, \tag{B5}$$

where

$$\epsilon(\theta) = \frac{1}{\sqrt{\left(\dfrac{\cos^2\theta}{\epsilon_2} + \dfrac{\sin^2\theta}{\epsilon_1}\right)\left(\dfrac{\cos^2\theta}{\epsilon_3} + \dfrac{\sin^2\theta}{\epsilon_1}\right)}}. \tag{B6}$$

The integration in Eq. (B5) can be represented in terms of the hypogeometric function ${}_2F_1$ as

$$I = \frac{\pi}{2}\frac{1}{\sqrt{\epsilon^2(\theta)\epsilon_2\epsilon_3}}\frac{\sqrt{\epsilon(\theta)}}{\sqrt[4]{\epsilon_2\epsilon_3}}{}_2F_1\left(\frac{1}{2}, \frac{1}{2}, 1; \frac{-(\epsilon_2 - \epsilon_3)^2}{4\sqrt{\epsilon_2\epsilon_3}}\right) \tag{B7}$$

therefore

$$\epsilon_{\|}^{d}(\theta) = {}_2F_1 \sqrt[4]{\frac{\epsilon_2\epsilon_3}{\left(\frac{\sin^2\theta}{\epsilon_1}+\frac{\cos^2\theta}{\epsilon_2}\right)\left(\frac{\sin^2\theta}{\epsilon_1}+\frac{\cos^2\theta}{\epsilon_3}\right)}}. \tag{B8}$$

When $\epsilon_2=\epsilon_3$ then ${}_2F_1(\frac{1}{2},\frac{1}{2},1;0)=1$ and the expression for $\epsilon_{\|}^{d}(\theta)$ reduces to

$$\epsilon_{\|}^{d}(\theta) = \epsilon_2 \sqrt{\frac{\epsilon_1}{\epsilon_1\cos^2\theta+\epsilon_2\sin^2\theta}} \tag{B9}$$

in agreement with Ref. [12]. If the dipoles are randomly oriented then the average value of the dielectric constant is given by

$$\overline{\epsilon^d} = \frac{1}{2}\int_0^{\pi}\epsilon_{\perp}^{d}(\theta)\sin\theta d\theta = \frac{1}{2}\int_0^{\pi}\epsilon_{\|}^{d}(\theta)\sin\theta d\theta. \tag{B10}$$

APPENDIX C: HARD-SPHERE DIAMETER, LENNARD-JONES WELL DEPTH, AND DIPOLE MOMENT

The hard sphere diameter σ, Lennard-Jones interaction well depth u_0, and dipole moment m in a particular solvent are required in the calculation of the reduced dipole moment, Eq. (6). We discuss the determination of these quantities in this appendix.

There are two methods for calculating the hard-sphere diameter σ which can lead to significantly different values for this parameter. In Table I we have usually represented σ by a range in values determined by these two methods. The hard-sphere diameter of a molecule can be calculated using Eq. (7.1) in Ref. [5]

$$\frac{\sigma}{2} = 0.463 b^{1/3}, \tag{C1}$$

where b is the van der Waals equation of state coefficient (in dm^3/mol) and σ is in nm. This expression provides the smallest value for σ. It reflects the size of the molecule during a collision; this size is smaller than the equilibrium separation. The hard-sphere σ can also be calculated from the mean molecular volume of the liquid $v=M/\rho N_0$ where M is the molecular weight, ρ is the mass density, and N_0 is Avogadro's number using Eq. (7.2) in Ref. [5]

$$\frac{4}{3}\pi\left(\frac{\sigma}{2}\right)^3 = 0.7405 v. \tag{C2}$$

This method provides the highest value for σ. For 2-nitroanisole the literature value for b could not be found and σ has only been calculated from Eq. (C2).

The interaction well depth u_0, between two neutral dipoles, can be estimated by comparing the attractive potential of Frodl and Dietrich [13], $4u_0(\sigma/r)^6$, with the corresponding expression for the total van der Waals interaction $w(r)$ that decays proportional to r^{-6} [46]. For two identical molecules 1 in a medium 2 then from Eq. (6.35) in Ref. [5]

$$w(r) \approx -\left[3k_BT\left(\frac{\epsilon_1(0)-\epsilon_2(0)}{\epsilon_1(0)+2\epsilon_2(0)}\right)^2 + \frac{\sqrt{3}h\nu_e}{4}\frac{(\epsilon_1-\epsilon_2)^2}{(\epsilon_1+2\epsilon_2)^{3/2}}\right]\frac{a_1^6}{r^6}, \tag{C3}$$

where $\epsilon_i(0)$ and $\epsilon_i(i=1,2)$ are, respectively, the static and optical dielectric constants and we have assumed that $a_1=\sigma$. Provided a material can be well characterized by a single dominant uv absorption frequency, the frequency ν_e can be determined from a Cauchy plot [21] if the refractive index is known as a function of frequency in the visible region. We assume in this paper that ν_e possesses a $\pm 10\%$ error in this calculation. For example, for 2-nitroanisole we estimate that $\nu_e=(1.8\pm 0.18)\times 10^{15}$ Hz from a Cauchy plot for the molecule nitrobenzene using the refractive index data in Ref. [47]. Nitrobenzene and 2-nitroanisole possess a similar structure and therefore they are expected to have similar ν_e values. From Eq. (C3) we therefore obtain $u_0=(2.68-2.83)\times 10^{-21}$ J for 2-nitroanisole.

The dipole moment m of certain molecules depends upon their environment. The gas phase value ($m_{\rm gas}$) may differ substantially from the value acquired in a solvent ($m_{\rm sol}$) where the correction factor depends upon the solvent dielectric constant and upon the structure of the polar molecule [48]. We have used the Higasi expression in Ref. [48] to determine the ratio

$$R = \frac{m_{\rm sol}}{m_{\rm gas}} = 1+\left(\xi-\frac{1}{3}\right)(\epsilon_s-1)/\epsilon_s, \tag{C4}$$

where the solvent medium is assumed isotropic and the polar molecule is modeled as an ellipsoid with dipole moment parallel to one of the principal axes. Here ϵ_s is the solvent dielectric constant and the internal field function ξ can be calculated using Ref. [48]. ξ depends upon the axial ratios of the ellipsoid which is roughly proportional to the polarizabilities of the molecule in the corresponding directions. The theory implies that $R<1$ for prolate spheroids and $R>1$ for oblate spheroids. Most molecules possess a larger dielectric constant along the dipole axis compared with perpendicular to the dipole axis therefore normally $m_{\rm sol}<m_{\rm gas}$. For 2-nitroanisole in the solvent cyclohexane, from the polarizability data in Appendix A, we estimate that $R=0.935$ (which is similar to the values listed in Table I of Ref. [48]). Therefore from $m_{\rm gas}=4.83D$ [49] the dipole moment of 2-nitroanisole in the solvent cyclohexane is $m_{\rm sol}\approx 4.51D$. Hence from the information given in this appendix the dipolar molecule 2-nitroanisole possesses a reduced dipole moment $m^*=m/\sqrt{\sigma^3 u_0}$ in the range from 1.59 to 1.64 as listed in Table I.

[1] S. Chandrasekhar, *Liquid Crystals* (Cambridge University Press, New York, 1977).
[2] T.J. Sluckin and A. Poniewierski, in *Fluid Interfacial Phenomena*, edited by C.A. Croxton (Wiley, New York, 1986).
[3] B. Groh and S. Dietrich, Phys. Rev. E **53**, 2509 (1996); in *New Approaches to Problems in Liquid State Theory*, edited by C. Caccamo *et al.* (Kluwer, Dordrecht, 1999).
[4] W.H. Keesom, Phys. Z. **22**, 129 (1921).
[5] J.N. Israelachvili, *Intermolecular and Surface Forces*, 2nd ed. (Academic, London, 1992).
[6] S.A. Safran, *Statistical Thermodynamics of Surfaces, Interfaces, and Membrane* (Addison-Wesley, Reading, 1994).
[7] J.-P. Carton and Ludwik Leibler, J. Phys. (France) **51**, 1683 (1990).
[8] J.D. Jackson, *Classical Electrodynamics*, 2nd ed. (Wiley, New York, 1993).
[9] A.A. Maryott and E.R. Smith, *Table of Dielectric Constants of Pure Liquids*, National Bureau of Standards (U.S.), Circ. No. 514 (U.S. GPO, Washington, D.C., 1951).
[10] R. Superfine, J.Y. Huang, and Y.R. Shen, Phys. Rev. Lett. **66**, 1066 (1991); M.C. Goh, J.M. Hicks, K. Kemnitz, G.R. Pinto, K. Bhattacharyya, K.B. Eisenthal, and T.F. Heinz, J. Phys. Chem. **92**, 5074 (1988).
[11] E. Chacon, P. Tarazona, and G. Navascues, J. Chem. Phys. **79**, 4426 (1983); J. Eggebrecht, K.E. Gubbins, and S.M. Thompson, *ibid.* **86**, 2286, 2299 (1987); P.I. Teixeira, B.S. Almeida, M.N. Telo da Gamma, J.A. Rueda and R.G. Rubio, J. Phys. Chem. **96**, 8488 (1992).
[12] C.L. Caylor, B.M. Law, P. Senanayake, V.L. Kuzmin, V.P. Romanov, and S. Wiegand, Phys. Rev. E **56**, 4441 (1997).
[13] P. Frodl and S. Dietrich, Phys. Rev. E **45**, 7330 (1992); **48**, 3741 (1993).
[14] A. Mukhopadhyay, C.L. Caylor, and B.M. Law, Phys. Rev. E **61**, R1036 (2000).
[15] J.P. Hansen and I.A. McDonald, *Theory of Simple Liquids* (Academic, London, 1986).
[16] B. Widom, J. Phys. Chem. **100**, 13190 (1996).
[17] I. Szleifer and B. Widom, J. Phys. Chem. **90**, 7524 (1989).
[18] P.I. Teixeira and M.M. Telo da Gama, J. Phys.: Condens. Matter **3**, 111 (1991); B. Yang, D.E. Sullivan, B. Tjipto-Margo, and C.G. Gray, *ibid.* **3**, F109 (1991).
[19] T.J. Sluckin, Mol. Phys. **47**, 267 (1982); **43**, 817 (1981).
[20] J.S. Rowlinson and B. Widom, *Molecular Theory of Capillarity* (Clarendon, Oxford, 1982).
[21] R.F. Kayser, Phys. Rev. B **34**, 3254 (1986).
[22] S. Fisk and B. Widom, J. Chem. Phys. **50**, 3219 (1969).
[23] D. Beaglehole, in *Fluid Interfacial Phenomena*, edited by C. A. Croxton (Wiley, New York, 1986).
[24] D. Beaglehole, Physica B **100**, 163 (1980).
[25] A.M. Marvin and F. Toigo, Phys. Rev. A **26**, 2927 (1982).
[26] V.L. Kuzmin and V.P. Romanov, Phys. Rev. E **49**, 2949 (1994).
[27] M.E. Fisher and J.-H. Chen, J. Phys. (Paris) **46**, 1645 (1985).
[28] J.W. Schmidt, Phys. Rev. A **38**, 567 (1988).
[29] D.G. Miles, Jr. and J.W. Schmidt, J. Chem. Phys. **92**, 3881 (1990).
[30] J.W. Schmidt and M.R. Moldover, J. Chem. Phys. **99**, 582 (1993).
[31] W.R. Fawcett, Mol. Phys. **86**, 715 (1995).
[32] D.S.P. Smith, B.M. Law, M. Smock, and D.P. Landau, Phys. Rev. E **55**, 620 (1997).
[33] Beaglehole Instruments, URL http://www.beaglehole.com
[34] J.M.H. Levelt Sengers and J.A. Given, Mol. Phys. **80**, 899 (1993).
[35] A. Kumar, H.R. Krishnamurthy, and E.S.R. Gopal, Phys. Rep. **98**, 57 (1983).
[36] L.W. DaMore and D.T. Jacobs, J. Chem. Phys. **97**, 464 (1992).
[37] All numbers used for the polarizability calculation have been taken from J.O. Hirschfelder, C.F. Curtiss, and R.B. Bird, *Molecular Theory of Gases and Liquids* (Wiley, New York, 1954), Sec. 13.2.
[38] S.G. Grubb *et al.*, Langmuir **4**, 452 (1988).
[39] M. Schlossman (private communication); D.M. Mitrinovic, A.M. Tikhonov, M. Li, Z. Huang, and M.L. Schlossman, Bull. Am. Phys. Soc. **45**, 733 (2000).
[40] P.K.L. Drude, *The Theory of Optics* (Dover, New York, 1959), p. 292.
[41] M.E. Fisher and P.-G. de Gennes, C. R. Seances Acad. Sci., Ser. B **287**, 207 (1978).
[42] J.H. Carpenter, B.M. Law, and D.S.P. Smith, Phys. Rev. E **59**, 5655 (1999).
[43] J.-H. Cho and B.M. Law, (unpublished).
[44] H. Hsiung, Th. Rasing, and Y.R. Shen, Phys. Rev. Lett. **57**, 3065 (1986); W. Chen, L.J. Martinez-Miranda, H. Hsiung, and Y.R. Shen, *ibid.* **62**, 1860 (1989).
[45] B.M. Ocko, A. Braslau, P.S. Pershan, J. Als-Nielsen, and M. Deutsch, Phys. Rev. Lett. **57**, 94 (1986).
[46] This equation is strictly valid only for $r \gg \sigma$ [5], however, it probably provides a reasonable estimate for u_0.
[47] J. Timmermans, *Physico-Chemical Constants of Pure Organic Compounds* (Elsevier, New York, 1950).
[48] I.G. Ross and R.A. Sack, Proc. Phys. Soc. London **63**, 893 (1950).
[49] *Handbook of Chemistry and Physics*, 66th ed., edited by R.C. Weast, M.J. Astle, and W.H. Beyer (CRC, Boca Raton, 1985).
[50] *Landolt-Bornstein, Zahlenwarte und Funktionen aus Physik, Chemie, Astronomie, Geophysik, und Tecknik*, 6th ed., Vol. 1, Pt. 3, (Springer-Verlag, Berlin, 1951), pp. 509-512.